TISSUE ENGINEERING: Part C
Volume 19, Number 10, 2013

DOI: 10.1089/ten.tec.2012.0651

Cell-Laden Poly(ε-caprolactone)/Alginate Hybrid Scaffolds Fabricated by an Aerosol Cross-Linking Process for Obtaining Homogeneous Cell Distribution: Fabrication, Seeding Efficiency, and Cell Proliferation and Distribution

HyeongJin Lee, MS,[1] SeungHyun Ahn, MS,[1] Lawrence J. Bonassar, PhD,[2] Wook Chun, MD,[3] and GeunHyung Kim, PhD[1]

Generally, solid-freeform fabricated scaffolds show a controllable pore structure (pore size, porosity, pore connectivity, and permeability) and mechanical properties by using computer-aided techniques. Although the scaffolds can provide repeated and appropriate pore structures for tissue regeneration, they have a low biological activity, such as low cell-seeding efficiency and nonuniform cell density in the scaffold interior after a long culture period, due to a large pore size and completely open pores. Here we fabricated three different poly(ε-caprolactone) (PCL)/alginate scaffolds: (1) a rapid prototyped porous PCL scaffold coated with an alginate, (2) the same PCL scaffold coated with a mixture of alginate and cells, and (3) a multidispensed hybrid PCL/alginate scaffold embedded with cell-laden alginate struts. The three scaffolds had similar micropore structures (pore size = 430–580 μm, porosity = 62%–68%, square pore shape). Preosteoblast cells (MC3T3-E1) were used at the same cell density in each scaffold. By measuring cell-seeding efficiency, cell viability, and cell distribution after various periods of culturing, we sought to determine which scaffold was more appropriate for homogeneously regenerated tissues.

Introduction

Tissue engineering is a rapidly growing interdisciplinary research area that may provide options for treating damaged tissues and organs. As a promising technique for regenerating various tissues, this technology requires biomedical scaffolds, which serve as an artificial extracellular matrix (ECM) to support neotissue growth.[1–3]

Generally, the scaffold should be processed into a three-dimensional (3D) shape because cells are sensitive to topographical differences between 2D and 3D structures.[4–6] According to Abbott *et al.*, cell activities in 3D scaffolds show more realistic cellular behavior than those observed in 2D scaffolds.[7,8] The 3D scaffold should also have controllable biodegradability and a reasonable pore structure of optimal pore size and distribution with 100% interconnected pores, allowing for facile communication between the cells dispersed in the scaffold, promoting cellular activities (proliferation and differentiation), and inducing rapid angiogenesis processes (blood vessel formation).[9,10] To fulfill these pore structure requirements, several types of scaffold fabrication methods, including solvent casting/particulate leaching, phase separation, gas foaming, freeze-drying, electrospinning, and solid freeform fabrications (SFFs) have been proposed.[11–22] Of these methods, SFFs, which can fabricate scaffolds with predetermined porosity and pore structures, have been widely used to prepare custom scaffolds. However, although the scaffolds fabricated using SFF have various advantages [controllable mechanical property and precisely repeatable pore structure (pore size and porosity)], they still have some drawbacks. These include a low initial cell-seeding efficiency, which results in nonhomogeneous cell proliferation and distribution within the scaffold after some culture periods.

To improve the cell-seeding efficiency and enhance homogeneous cell distribution, various strategies have been proposed. One approach involves the cell culture system. Generally, the typical cell-seeding methods are static or

[1]Department of Bio-Mechatronic Engineering, College of Biotechnology and Bioengineering, Sungkyunkwan University, Suwon, South Korea.
[2]Department of Biomedical Engineering, Cornell University, Weill Hall, Ithaca, New York.
[3]Department of Surgery, College of Medicine, Hallym University Burn Institute, Hallym Univeristy, Hangang Sacred Heart Hospital, Seoul, South Korea.

dynamic seeding. The static system is the most generally used method and cells can be injected on the surface of scaffolds. In contrast, dynamic seeding uses a medium flow that is controlled by various external tools, such as spinner flasks,[23] rotational bioreactors,[24] and perfusion.[25] As reported by Sailon *et al.*,[26] dynamic-seeding systems can provide a continuous medium flow across the surface of the scaffold, inducing higher cellular activities than those of static culture systems. However, although a dynamic seeding system can increase cell-seeding efficiency to some degree, the flow of medium does not fully penetrate within the microsized pore structure in the scaffold's interior; therefore, the medium does not provide significantly effective chemotransportation.[27,28]

Another approach involves the physical structure of the scaffolds. In a recent report, Sobral *et al.* sought to modify the internal microarchitecture of the scaffolds to overcome the low initial seeding efficiency and nonuniform cell proliferation.[29] They obtained a reasonable physical structure of the scaffold, which improved the initial cell-seeding efficiency from 35% to 70%. In addition, several researchers have suggested unique scaffolds to improve cell-seeding efficiencies and enhance homogeneous cell distribution.[22,29–31] Hierarchical scaffolds, which consist of microsized struts and electrospun nanofibers, provide a significantly higher cell-seeding efficiency, due to the embedded nanofibers. Moreover, coated scaffolds, which consist of rapid-prototyped poly(ε-caprolactone) (PCL) microsized struts and various coating materials, including collagen, β-tricalcium phosphate, and alginate, show improved seeding and biological properties (e.g., alkaline phosphatase activity and calcium deposition) as compared with pure PCL scaffolds.[32,33] Recently, to obtain homogeneous cell distribution in cultured scaffolds, we fabricated a highly porous cell-laden alginate 3D scaffold using an aerosol technique.[34] The scaffold showed homogeneous cell distribution with high cell viability ($\sim$85%) and good cell proliferation as compared with a conventional cell-printed scaffold. The fabricated scaffolds showed impressive cell-seeding efficiencies and cellular activities as compared with the control scaffolds. However, although each scaffold showed significant cellular activities (cell-seeding efficiency, cell viability, and cell distribution) after various periods of culturing, we sought to determine which scaffold was more appropriate for homogeneously regenerated tissues under a similar pore and chemical structure of the scaffolds.

In this work, we used two polymers, PCL and alginate. PCL is a semicrystalline aliphatic polyester that has been investigated as a prospective biomaterial for orthopedic applications due to its biocompatibility and slow degradation kinetics (2–4 years). However, PCL has a low cellular activity due to its hydrophobicity and low water-absorbing capacity.[35,36] Alginate, which is derived from brown seaweed, is a well-known anionic linear polysaccharide composed of 1,4-linked β-D-mannuronic (M) and a-α-guluronic acid (G) residues.[37] It has been used widely as a tissue regenerative material because it accelerates epithelialization and granular tissue formation, as well as encapsulates various growth factors, due to its rapid gelation in calcium chloride.[38,39] However, major problems associated with alginate use include its low mechanical strength and low 3D shapeability, which may limit its further use as a template for tissue regeneration.[40] By combining the advantageous properties (shapeability and good mechanical properties) of PCL and reinforcing the disadvantageous factors (low cellular responses) of the PCL with an alginate, we sought to fabricate hybrid scaffolds.

In general, the cell-dispensing method has been widely used to overcome nonhomogenous cell distribution in a scaffold. However, although this method can homogeneously fabricate various cell-laden scaffolds, there are several deficiencies, such as the noncontrollable micropore structure, realistic 3D shape, and low mechanical properties as a scaffold.

One of our goals was to fabricate homogenously cell-distributed scaffolds by using a simple coating method and a hybrid cell-dispensing technique. The cell-dispensing process supplemented with an aerosol method to tentatively cross-link dispensed cell-laden alginate struts was used to obtain a designed pore structure that consisted of cell-laden alginate and pure PCL struts in successive layers.

In this study, to achieve the goal, we fabricated three different scaffolds and compared biological activities, cell-seeding efficiency, cell viability, and cell distribution after several culture periods. The reason of the selection of the scaffolds was that the hybrid (PCL and cell-embedded alginate) scaffold and cell-coated PCL scaffolds can provide high mechanical properties as well as significantly improved cell distribution compared to those of the synthetic pure scaffold and pure cell-laden alginate scaffold.

The three scaffolds consisted of microsized PCL struts (a layer-by-layer structure) and an alginate as follows: (1) a rapid-prototyped PCL structure coated with an alginate and cells injected on the scaffold (a static seeding method), (2) the same PCL structure coated with a mixture of alginate and cells, and (3) a hybrid scaffold, consisting of PCL struts and cell-laden alginate struts, fabricated using the cell-dispensing process supplemented with an aerosol cross-linking process.

To avoid micropore structure effects of the scaffolds on cellular activities, we used a similarly sized internal microstructure [pore size between struts = 430–580 μm, square pore shape, porosity = 62%–68% in the apparent size ($10 \times 10 \times 1.7\,mm^3$) of the scaffold] and the same density of MC3T3-E1 cells (1×10^5 mL^{-1}). In this work, we fabricated three scaffolds with the same material (PCL and alginate) and the same cell density. These scaffolds were cultured with the same procedure, so that our other goal was to determine which of these three scaffolds was more appropriate to homogeneously regenerate tissues by measuring cell-seeding efficiency, initial cell viability, and cell distribution after culturing for 30 days.

Experimental

Materials and characterizations

PCL (Cat. No. 440 744, melting point = 60°C) was obtained from Sigma-Aldrich. PCL has an average molecular weight (M_n) of $60{,}000\,g \cdot mol^{-1}$. Low-viscosity, high G-content nonmedical grade LF10/60 alginate (FMC BioPolymer) was mixed with phosphate-buffered saline (PBS) to prepare 3.5 wt% alginate. To cross-link the alginate solution, $CaCl_2$ (Sigma-Aldrich) was used.

The structural morphology of the scaffolds was observed under an optical microscope (BX FM-32; Olympus) connected to a digital camera and a scanning electron microscope (SEM, Leica 440). The apparent porosity of the scaffolds was

obtained using the equation: Porosity (%) = (1–M/ρV) × 100, where M is the mass of the scaffold and V is the total scaffold cube volume, assumed to be a bulk surface. The density, ρ, of the scaffolds was obtained using the rule of mixtures.[32] To measure the mass (M), the samples were weighed with a precise balance (AB204-S, Mettler Toledo).

The fabricated scaffolds were cut into small strips ($10 \times 20\ mm^2$). A uniaxial test was performed using a tensile testing machine (Top-tech 2000; Chemilab). The stress–strain curves for the scaffolds were recorded at a stretching speed of $2\ mm \cdot s^{-1}$. All values are expressed as the mean ± standard deviation (SD) ($n = 5$).

Scaffold fabrication

To fabricate the three scaffolds (S-1, S-2, and S-3), three fabrication methods were used.

(1) S-1 Scaffold: A melt-plotting system connected to a three-axis robot and an alginate-coating process were used to fabricate a PCL/alginate scaffold that was coated with an alginate. PCL powder was injected into a heating cylinder at 110°C, and the melted PCL was plotted through a microsized nozzle (inner diameter, 250 μm) in a layer-by-layer manner. The ambient temperature was 27°C. The applied pneumatic pressure during the extrusion of the PCL was 350 ± 40 kPa. After fabricating the PCL structure, the scaffolds were coated with an alginate solution (3.5 wt%) using a syringe pump, and a suction process was applied to coat the PCL scaffold evenly. The coated PCL/alginate scaffold was dried in an incubator for 2 h. Finally, to cross-link the coated alginate layer, the dried scaffolds were immersed in a 2 wt% $CaCl_2$ solution, prepared in PBS. The final samples were washed five times with distilled water to remove any unreacted calcium chloride solution. Finally, cells were injected on the coated scaffold at a density of $1 \times 10^5\ mL^{-1}$.

(2) S-2 Scaffold: Using the previous melt-plotting method, the same PCL structure was fabricated. However, the scaffold was coated with a mixture of an alginate (3.5 wt%) and preosteoblast cells (cell density, $1 \times 10^5\ mL^{-1}$) without a suction process to sustain the cell density. The other procedures were as described in the previous method.

(3) S-3 Scaffold: Alginate was mixed with PBS to prepare 3.5 wt% alginate. Before loading the cells, the alginate solution was mixed with 0.5 wt% $CaCl_2$ to increase the viscosity of the solution (the ratio of the alginate and $CaCl_2$ solution was 7:3). Cells were mixed into the alginate solution using a three-way stopcock at a density of $1 \times 10^5\ mL^{-1}$. The cell–alginate mixture was loaded into a syringe barrel. Perpendicular PCL struts with 1-mm pore size were fabricated using the previous melt-plotter and the mixture of alginate and cells was plotted between the PCL struts. During plotting of the cell-laden alginate [nozzle size = 240 μm, moving speed of nozzle = $10\ mm \cdot s^{-1}$, pneumatic pressure (260 ± 23 kPa)], aerosols of the 5 wt% $CaCl_2$ solution (flow rate = $0.93 \pm 0.12\ mL \cdot min^{-1}$) were used to tentatively cross-link the plotted alginate. The detailed aerosol process was described in our previous report.[34] After obtaining the layer-by-layer structure of PCL and alginate with cells, a secondary cross-linking procedure was conducted with a 2 wt% $CaCl_2$ solution prepared in media for 1 min to completely cross-link the cell-alginate struts in the hybrid scaffold. The scaffold was then washed three times with PBS. In the finally fabricated PCL/alginate scaffold, the cell-laden alginate struts were displaced between the PCL struts with interdigitated structures. Detailed scaffold fabrication procedures for the S-1, S-2, and S-3 scaffolds are shown in Figure 1.

Cell-seeding efficiency

The scaffolds in 24-well plates were cultured during 12 h, and the scaffolds were removed, and the attached cells in the scaffolds and the remaining cells in the wells were

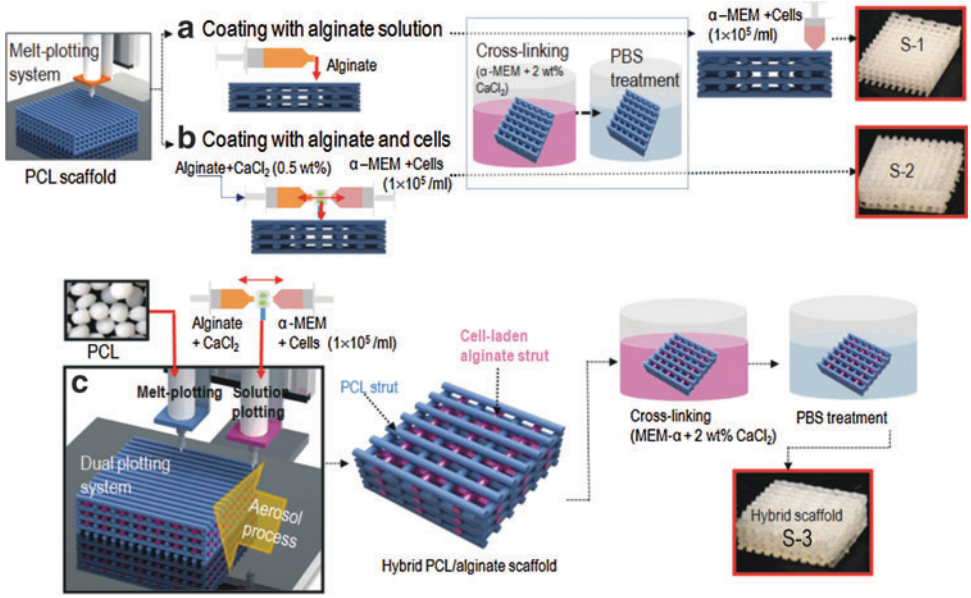

FIG. 1. Schematic of the fabrication procedures for the three scaffolds: **(a)** S-1, **(b)** S-2, and **(c)** S-3. Color images available online at www.liebertpub.com/tec

determined by 3-(4,5-dimethylthiazol-2-yl)-2,5-diphenyltetrazolium bromide (MTT) assay. The detail MTT assay was described in next following section. In this work, we assumed that the number of the initial injection cells indicated the total optical density (OD), which is the sum of OD of the scaffold and OD of the respective well. The ratio of the OD value of the scaffold to the total OD value was defined as the cell-seeding efficiency.

Fluorescence images and cell viability

After cell culture, the scaffolds were exposed to 0.15 mM calcein AM and 2 mM ethidium homodimer-1 for 45 min in an incubator to permit observation of live and dead cells. The stained specimens were analyzed under a microscope (TE2000-S; Nikon) equipped with an epifluorescence attachment and a SPOT RT digital camera (SPOT Imaging Solutions). Stained images were captured, in which green and red indicated live and dead cells, respectively.

To observe cell viability, we captured the images and processed the number of green and red spots using the ImageJ program (NIH). The ratio (cell viability) of the number of live cells to the total number of cells (including live and dead cells) was calculated using the ImageJ software.

In vitro *cell culture*

The scaffold (7 mm × 7 mm) was cultured and maintained in the α-minimum essential medium (Life Science) containing 10% fetal bovine serum (Gemini Bio-Products) and 1% antibiotic (Antimycotic; Cellgro). The cells were seeded onto the surface of the PCL scaffold coated with alginate at a density of 1×10^5 mL^{-1}. To allow attachment of the seeded cells, the scaffold without a medium was incubated for 4 h in an atmosphere of 5% CO_2 at 37°C. The medium was changed every second day. After 14 and 30 days of culture, the three scaffolds were analyzed with diamidino-2-phenylindole (DAPI) fluorescent staining to characterize the nuclei of the cells in the scaffold. Phalloidin (Invitrogen, Inc.) was used to visualize the actin cytoskeletons of proliferated cells in the scaffolds. Fluorescence images were acquired with a fluorescence microscope (Zeiss observer. z1; Zeiss). The proliferation of viable cells was determined using the MTT cell proliferation assay (Cell Proliferation Kit I; Boehringer Mannheim). This assay is based on the cleavage of the yellow tetrazolium salt, MTT, by mitochondrial dehydrogenases in viable cells to produce purple formazan crystals. Cells on the surface were incubated with 0.5 $mg \cdot mL^{-1}$ MTT for 4 h at 37°C. The absorbance at 570 nm was measured using a microplate reader (EL800; Bio-Tek Instruments). Four samples were tested for each incubation period, and each test was performed in triplicate.

After 30 days of cell culture, the scaffolds were analyzed with DAPI fluorescent stain to characterize the nuclei of the cells in the scaffold. Phalloidin (Invitrogen) was used to visualize the actin cytoskeletons of proliferated cells in the scaffolds. The cell number identified by DAPI-stained cell nuclei was counted using ImageJ from the cross-sectional fluorescence images of the scaffolds. The number of cells for each region (top, middle, and bottom of the scaffolds) was normalized with total number of cells and it was defined as the cell uniformity of the scaffold.

Statistical analyses

All data are presented as means ± SD. Statistical analyses were performed using the SPSS software (ver. 20.0; SPSS, Inc.). Statistical analyses consisted of single-factor analyses of variance (ANOVAs). In all analyses, $*p < 0.05$ was taken to indicate statistical significance. 'NS' indicates nonsignificant.

Results and Discussion

The efficiency of an aerosol cross-linking process for fabricating cell-laden PCL/alginate scaffolds

In the cell-dispensing process, the controllability of the strut diameter is an important fabrication parameter because the size sustainability of the struts can significantly affect the designed pore size of the final cell-laden scaffold. To show the feasibility of the aerosol cross-linking process in the cell-dispensing process, we simply tested the size change of the dispended alginate struts with and without the aerosol fuming process. The flow rate of the aerosol solution of $CaCl_2$ was fixed at 0.93 ± 0.12 $mL \cdot min^{-1}$. A nozzle size of the dispenser was 310 μm. Cells were mixed with various weight fractions (2, 3.5, and 5 wt%) of the alginate solution at a density of 1×10^5 mL^{-1}. Figure 2(a) and (b) show the surface and cross-sectional optical images of cell-laden alginate struts dispensed over the PCL struts, respectively. As shown in the images, the cell-laden alginate struts cross-linked with the aerosols of $CaCl_2$ showed a significantly stable size compared to the struts without the process [Fig. 2(c)]. As shown in Figure 2(d), the percent of the size reduction, ([alginate strut-size w/o an aerosol process]–[alginate strut-size with an aerosol process])/(alginate strut-size w/o an aerosol process) × 100, for various weight fractions of alginate (2, 3.5, and 5 wt%) was roughly 35% ± 7%. From the results, we can find that the aerosol cross-linking process can highly influence the designing of the pores in the 3D cell-laden hybrid scaffolds.

Scaffold fabrication and morphological characterizations of scaffolds

In this work, we fixed the pore size at 500 μm because a pore size over 300 μm is recommended for osteoconduction and vascularization.[41] Figure 2 shows optical, fluorescence, and SEM images of the pure PCL scaffold [Fig. 3(a)] and the three scaffolds: S-1, PCL coated with the alginate solution [Fig. 3(b)]; S-2, PCL coated with a mixture of alginate and cells [Fig. 3(c)]; and S-3, interdigitated PCL/alginate struts in which cells were embedded in the alginate struts [Fig. 3(d)].

As shown in Figure 3(a), a layer-by-layer pore structure (pore size = 579 ± 12 μm) of the pure PCL scaffold was achieved. When comparing the pore structure of the pure PCL scaffold and the scaffolds coated with the alginate solution and alginate/cells [Fig. 3(b, c)], the scaffold coated with the alginate solution slightly blocked the circumference of the square pores. However, the coated PCL scaffolds still had sufficient pore size and open pores to induce cell proliferation to the thickness of the scaffold. In addition, as shown in Figure 3(d), the hybrid PCL/alginate scaffold, laden with cell-alginate struts, showed a homogeneous pore size and 100% pore interconnectivity. Although the pore size was slightly reduced from the original pure PCL architecture, the sizes of most of the pores for all of the scaffolds

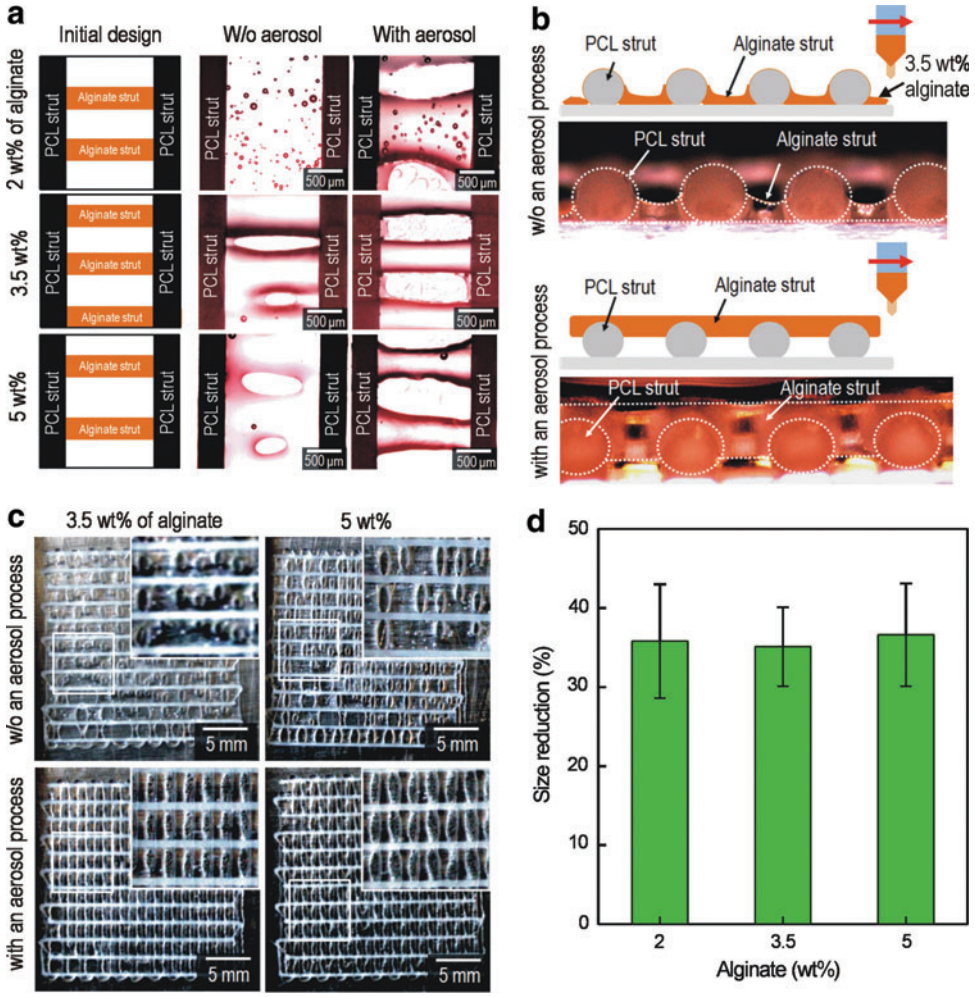

FIG. 2. The optical images of cell-laden alginate struts with and without an aerosol process, **(a)** surface, and **(b)** cross-sectional images. **(c)** The dispensed alginate struts (3.5 and 5 wt% of alginate with cells) over the poly(ε-caprolactone) (PCL) struts with and without an aerosol process. **(d)** The percent of the size reduction, ([alginate strut-size w/o an aerosol process]–[alginate strut-size with an aerosol process])/(alginate strut-size w/o an aerosol process)×100, for various weight fractions of alginate (2, 3.5, and 5 wt%). Color images available online at www.liebertpub.com/tec

were over 400 μm. In addition, the surface and cross-sectional fluorescence images show that the embedded cells are well distributed and live (green color). The detailed pore sizes, strut sizes, and porosity of the pure PCL and three scaffolds are described in Table 1.

Mechanical properties

The mechanical properties of the scaffold are an important parameter for the biological activities of cells, because the cells can sense the mechanical strength of the scaffold, so that low mechanical properties can induce low attachment and proliferation of cells.[42–44] Ordinarily, the mechanical properties of a SFF structure can be readily controlled by its microporous structures (strut diameter, pore size, porosity, and orientation of struts). For these reasons, to avoid the effects of the mechanical properties of scaffolds on cellular activity, we sought to fabricate similar micropore structures in all of the scaffolds.

Figure 4(a) shows the stress–strain curves of the three scaffolds. The mechanical analysis was conducted using the tensile mode for a constant stretching speed of $2.0\,mm\cdot s^{-1}$. As expected, the S-3 scaffold showed the lowest tensile strength curve, due to the low volume fraction of PCL and cell-laden alginate struts in the scaffold. The S-1 and S-2 scaffolds showed similar mechanical properties because of their similar PCL structures. Figure 4(b) shows the comparisons of the elastic modulus and maximum strength for the three scaffolds. As shown in the figure, the moduli of the scaffolds (S-1 and S-2), ranging from 4.1 to 5.1 MPa, were approximately similar to that of the pure PCL structure (4.5 ± 0.7 MPa) for the given stretching speed. Statistical analysis using a one-way ANOVA indicated no significant difference ($^*p > 0.05$) among the moduli of the S-1 and S-2 scaffolds. This indicates that the coated alginate did not affect the mechanical properties of the PCL/alginate scaffolds, due to the low mechanical nature of the alginate, while the S-3 scaffold showed a relatively low tensile modulus (3.5 ± 0.4 MPa) due to the relatively low volume percentage of PCL struts in S-3. This can be analyzed simply with the rule of mixture, ($E_T = E_P\phi_P + E_a\phi_a$), where E_P (4.5 MPa) and E_a (0.5 MPa) are the moduli of pure PCL and pure alginate, measured using the same tensile testing condition, respectively, and ϕ_P (65%) and ϕ_a (35%) are the volume fractions of the PCL and alginate of the S-3 scaffold, respectively. The volume fractions of PCL and alginate were calculated using the numbers of each strut, assuming that the strut was a completely cylindrical shape. Through this simple analysis, the calculated modulus for the S-3 scaffold was obtained as 3.1 MPa. This value was slightly below the measured one

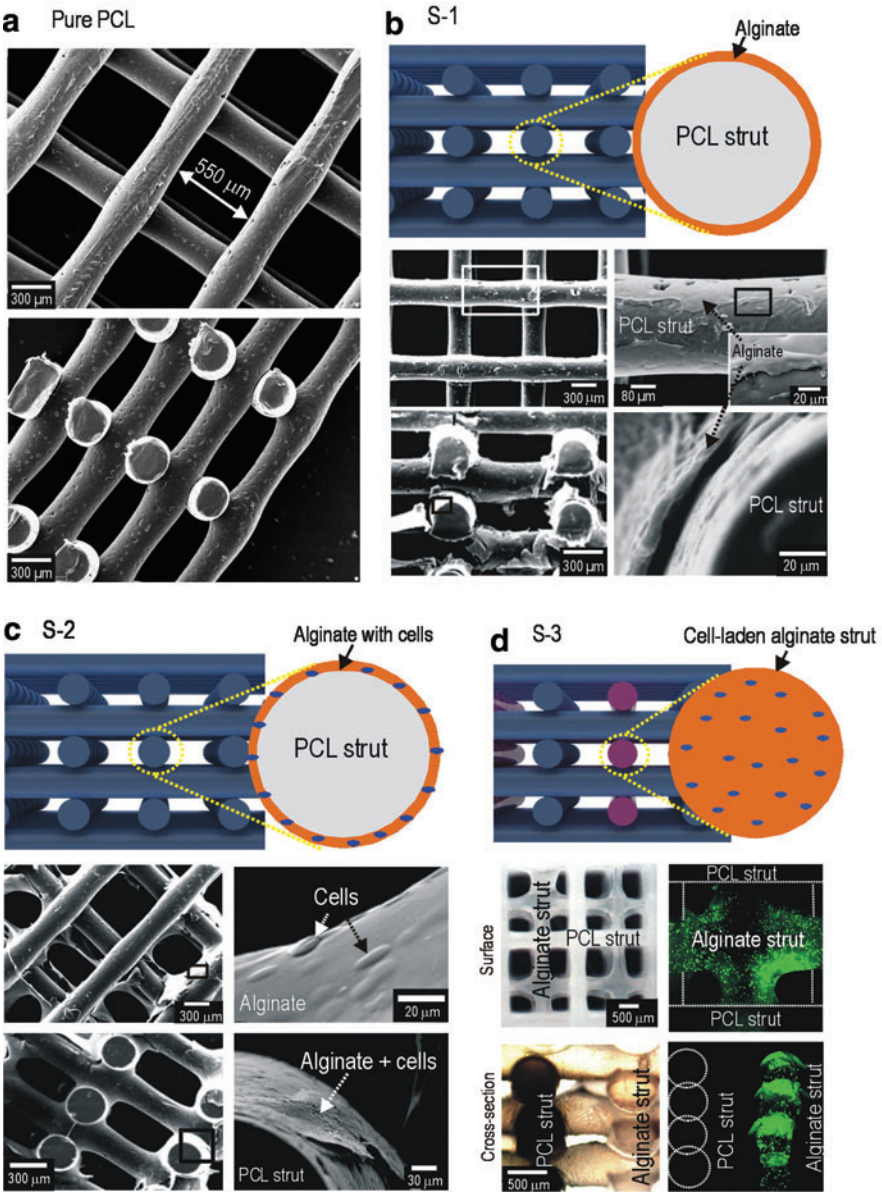

FIG. 3. Surface and cross-sectional scanning electron microscopy and optical images. **(a)** Pure PCL structure, **(b)** S-1 scaffold coated with the alginate solution (3.5 wt%), **(c)** S-2 scaffold coated with a mixture of alginate (3.5 wt%) and cells (MC3T3-E1, 1×10^5 mL^{-1}), and **(d)** S-3 scaffold consisting of pure PCL struts and cell-laden alginate struts (1×10^5 mL^{-1}). Color images available online at www.liebertpub.com/tec

(3.5 MPa), but considering the calculation assumptions, the difference between the measured and calculated moduli was insignificant.

In terms of mechanical properties, we can see that the mechanical properties of the alginate-coated scaffolds (S-1 and S-2) were similar, but the mechanical properties of the S-3 scaffold were relatively low (about 30% in the modulus) compared to those of the S-1 and S-2 scaffolds. However, if we consider the low mechanical properties of pure alginate, the mechanical properties of the S-3 scaffold were quite high.

Cell-seeding efficiency

Generally, cell-seeding efficiency can greatly influence tissue formation, uniformity of regenerated tissue, and even differentiation of cells.[45,46] To observe cell-seeding efficiency,

Table 1. Strut Diameter, Pore Size, and Porosity for Pure PCL Structure and the Three Scaffolds

				S-3	
	PCL structure	*S-1*	*S-2*	*PCL*	*Cell-laden alginate strut*
Strut diameter (μm)	251 ± 26	277 ± 25	281 ± 24	445 ± 28	436 ± 45
Pore size (μm)	579 ± 12	575 ± 12	546 ± 52		430 ± 66
Porosity (%)	68.9	68.2	67.6		62.6

PCL, poly(ε-caprolactone).

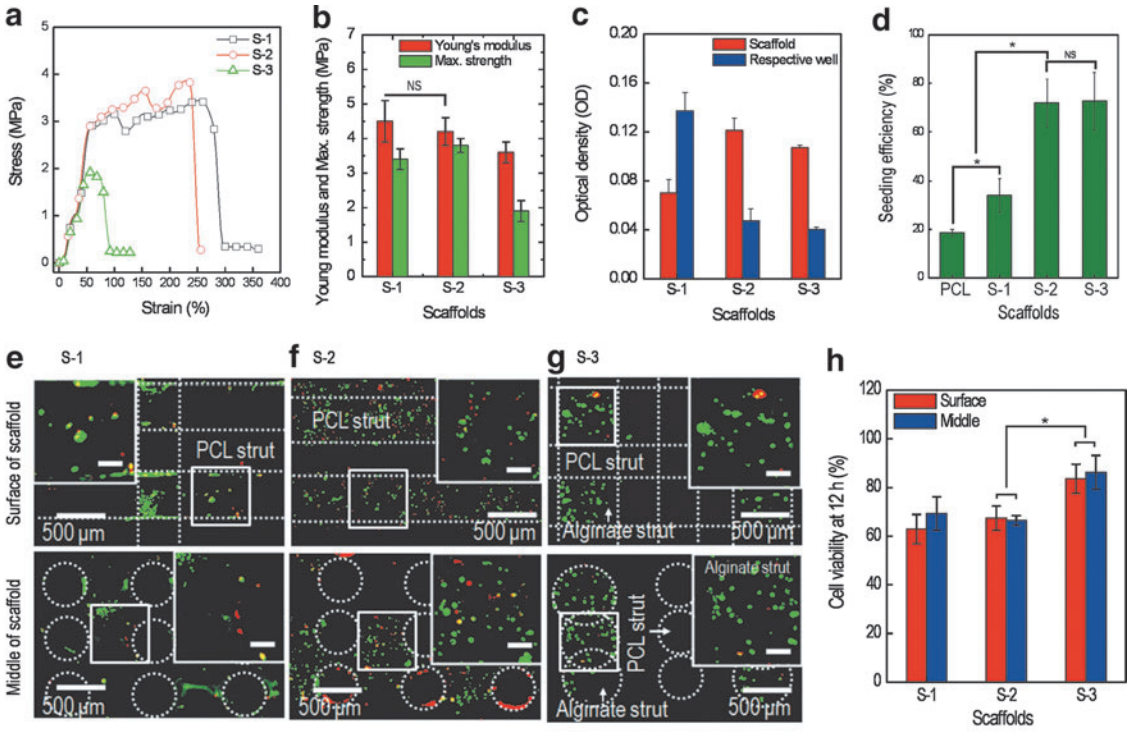

FIG. 4. **(a)** Stress–strain curves for the three scaffolds (S-1, S-2, and S-3). **(b)** Young's modulus and maximum strength ($n=5$). **(c)** Optical density (OD) as determined using the 3-(4,5-dimethylthiazol-2-yl)-2,5-diphenyltetrazolium bromide (MTT) assay after 12 h for scaffolds and respective wells and **(d)** cell-seeding efficiency (%); ([OD value of cells in scaffold] × 100)/total OD value, for the scaffolds. *$p<0.05$ and NS indicate a significant difference and nonsignificance, respectively. Fluorescence images of the surface and interior regions of scaffolds showing live (green) and dead (red) cells after 12 h in culture on **(e)** S-1, **(f)** S-2, and **(g)** S-3 scaffolds. **(h)** Comparison of initial cell viability (12 h) for surface and interior regions of the scaffolds. The scale bar in the magnified images indicates 100 μm. *$p<0.05$ and NS indicate a significant difference and nonsignificance, respectively. Color images available online at www.liebertpub.com/tec

the numbers of cells attached in the scaffolds and residual cells in the respective wells after culturing for 12 h with seeding (S-1), coating (S-2), and fabricating (S-3) were used. Figure 4(c) shows the OD, as determined using the MTT assay, after 12 h for scaffolds and respective wells. The cell-seeding efficiency was defined as the ratio of the OD of the scaffold to the total OD value (the OD value of scaffolds + OD value of the respective well). Figure 4(d) shows the seeding efficiency for the scaffolds. The seeding efficiencies of S-2 and S-3 were ~72.0% ± 10% and 72.8% ± 12%, respectively. The values for S-2 and S-3 were quite high versus that of the S-1 scaffold (conventional static cell-seeding method), which was ~33.8% ± 7%, because the cells in the S-2 and S-3 can become fixed with the mixed alginate or alginate struts. Although the hydrophobic surface of PCL (seeding efficiency for the pure PCL scaffold = 18.7%) was changed to a hydrophilic surface by the coated alginate solution, the S-1 scaffold showed the lowest cell-seeding efficiency, due to the larger pore size and open pores within the scaffold. This result was validated by live cell images, as in Figure 4(e–g), which were taken after 12 h in culture. As shown in the figures, live cells numbers with the S-2 and S-3 scaffolds were significantly higher than that with the S-1 scaffold.

Additionally, we expected a much higher seeding efficiency for the S-2 and S-3 scaffolds, but unlike our expectations, both the S-2 and S-3 scaffolds showed relatively low-seeding efficiencies. We estimate that this may have been because cells attached near the surface of the coated alginate and alginate struts may become detached from the surface.

Initial cell viability, MTT assay, and cell distribution

Initial cell viability is an important parameter for successful tissue regeneration using a scaffold because it greatly affects cellular activities, including proliferation and distribution of cells in the scaffold and tissue-regenerating time. To observe cell viability, live and dead cells were analyzed 12 h after seeding. To acquire images of live and dead cells, the scaffolds were stained with calcein AM and ethidium homodimer 1, respectively. Figure 4(e–g) shows fluorescent images of the scaffolds (S-1, S-2, and S-3, respectively), where live cells are green and dead cells are red. Using the fluorescence images, initial cell viability was measured with the number of live and dead cells. Figure 4(h) shows the comparison of cell viability of scaffolds after 12 h. Interestingly, the initial viability of S-1 (62.9% ± 6%) and S-2 (67.4% ± 5%) was relative low as compared with that of S-3 (83.6% ± 7%). We cannot completely explain this result, but we can estimate that the cell-attaching process with the S-1 scaffold during the initial 4 h without a medium may have caused damage to the injected cells. Regarding cell viability with S-2, the calcium chloride solution (the cross-linking agent of alginate) may have damaged

cells, because the protruding cells on the thin alginate, as seen in Figure 3(c), can directly contact the calcium chloride solution. However, for the S-3 scaffold, the alginate struts ($436 \pm 45\,\mu m$) can protect the cells embedded within it, although the curing solution may slightly interact with cells at the alginate surface.

To quantitatively observe the proliferation of viable cells, MTT assays were used [Fig. 5(a)]. Viable cells on the scaffolds proliferated with time, and at day 1, the OD value was higher in the S-2 and S-3 scaffolds than in the S-1 scaffold. This may be related to the cell-seeding efficiency. However, the proliferation rate of S-1 was higher than the cells on the S-2 and S-3 scaffolds. We believe this was because the cells attached on the S-1 scaffold could more freely proliferate on the surface of struts, while the cells bound with the alginate in the S-2 and S-3 scaffolds could not proliferate so easily. However, although the S-2 and S-3 scaffolds provided slightly lower proliferation rates as compared with S-1, the cells were still proliferating.

According to several researchers, to be able to obtain ultimate functionality as a tissue regenerative substitute, a biomedical scaffold should achieve homogeneous cell distribution in its interior structure.[47,48] Generally, the MTT assay results do not completely represent the cell distribution; therefore, we measured the cell distribution for various regions (top, middle, and bottom region of the cross section of the scaffolds) of the three scaffolds.

Figure 5 (b)–(d) show fluorescence images after 30 days of scaffold culture (S-1, S-2, and S-3), and the stained nuclei and F-actin in the images are shown in blue and red, respectively. As seen in the surface and cross-sectional images, the cells with the ECM proliferated well, and, in particular, for cross-sectional images, the cells grew between the pores during the culture period for each scaffold.

Although the cells proliferated in all scaffolds, the S-3 scaffold, which has interdigitated PCL and alginate struts embedded with cells, showed a very homogeneous cell distribution over the long culture period, versus the S-1 scaffold [Fig. 5(e)]. The S-2 scaffold also showed a quite homogeneous proliferated cell distribution. We believe the homogenous cell distribution in the S-3 scaffold was because of the cell-laden alginate struts in the scaffold, which can act as a cell reservoir to continuously release cells over the long culture period.

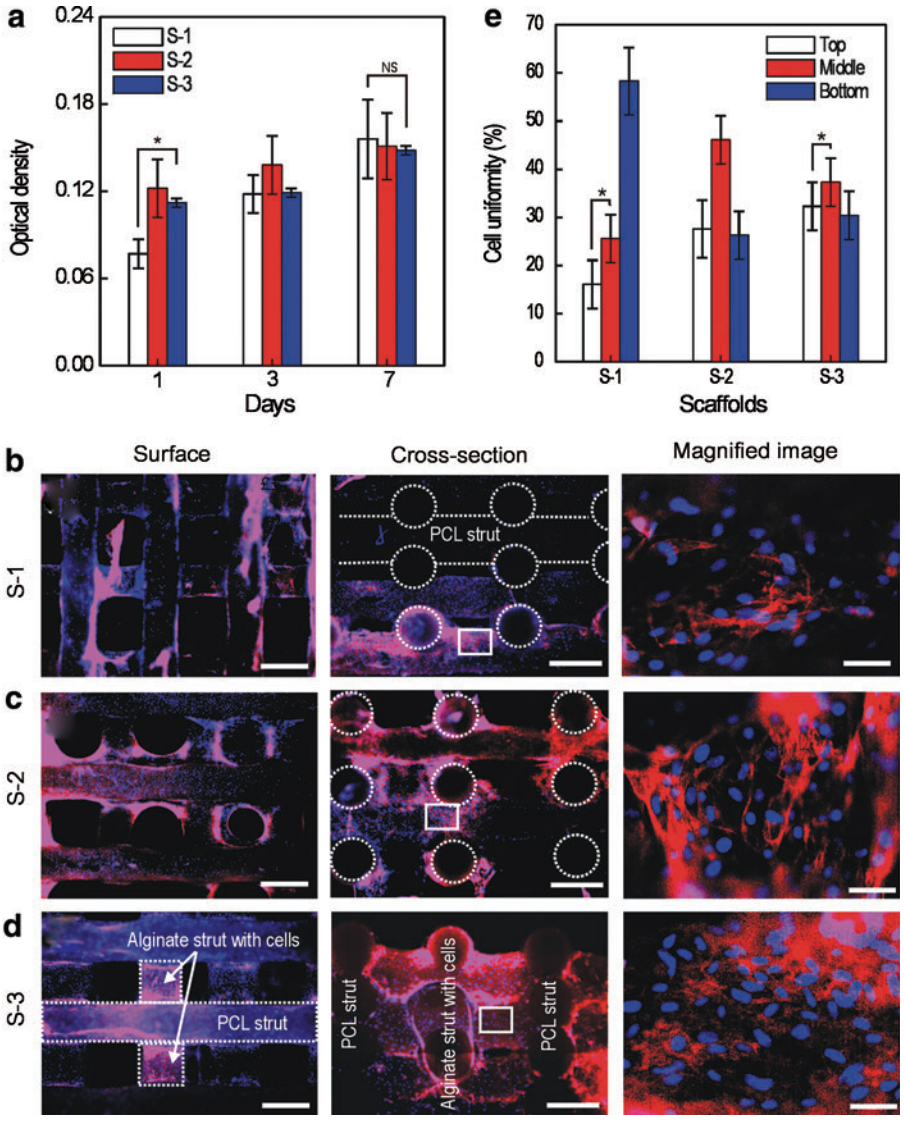

FIG. 5. **(a)** MTT assay result after 1, 3, and 7 days of scaffold culture (S-1, S-2, and S-3). $*p < 0.05$ and NS indicate a significant difference and nonsignificance, respectively. Fluorescence surface and cross-sectional images for the **(b)** S-1, **(c)** S-2, and **(d)** S-3 scaffolds after 30 days in culture. In this image, nucleus (blue) and F-actin (red). **(e)** Cell density for three regions (top, middle, and bottom) of the scaffolds. $*p < 0.05$ indicates a significant difference. In the surface and crosssectional images, the scale bar means 500 μm. The scale bar in the magnified image is 30 μm. Color images available online at www.liebertpub.com/tec

Conclusions

In this study, we fabricated three cell-laden scaffolds: a general rapid-prototyped PCL/alginate scaffold (S-1), a cell-coated PCL/alginate scaffold (S-2), and a hybrid PCL/alginate scaffold laden with alginate cells (S-3). All scaffolds had similar microarchitectures (pore size, pore shape, porosity, and open pores) to avoid effects of the pore structure on cellular behaviors, such as cell-seeding efficiency, proliferation, and distribution. Regarding cell-seeding efficiency, S-2 and S-3 showed significantly higher values than S-1, while cell proliferation in these scaffolds was slightly lower than that in S-1. Regarding cell distribution after a long cell culture period, the S-3 scaffold showed dramatically homogeneous cell density over the entire region of the scaffold as compared with the other scaffolds. This was because the cells from the cell-laden alginate struts in the scaffold could be released continuously, acting as a tentative cell reservoir. Based on the results of the biological activities, we confirmed that the S-3 scaffold, having cell-laden alginate struts, showed the highest cellular behavior, although the mechanical properties were relatively low versus the S-1 and S-2 scaffolds due to the inserted cell-laded alginate struts.

Acknowledgments

This study was supported by a grant from the Korea Healthcare Technology R&D Project, Ministry for Health, Welfare and Family Affairs, Republic of Korea (Grant no. A084589) and also was supported by the National Research Foundation of Korea grant funded by the Ministry of Education, Science, and Technology (MEST) (Grant no. 2012-0140).

Disclosure Statement

No competing financial interests exist.

References

1. Langer, R., and Vacanti, J.P. Tissue engineering. Science **260,** 920, 1993.
2. Peter, S.J., Miller, M.J., Yasko, A.W., Yaszemski, M.J., and Mikos, A.G. Polymer concepts in tissue engineering. J Biomed Mater Res **43,** 422, 1998.
3. Cima, L.G., Vacanti, J.P., Vacanti, C., Ingber, D., Mooney, D.J., and Langer, R. Tissue engineering by cell transplantation using degradable polymer substrates. J Biomech Eng **113,** 143, 1991.
4. Place, E.S., Evans, N.D., and Stevens, M.M. Complexity in biomaterials for tissue engineering. Nat Mater **8,** 457, 2009.
5. Chatterjee, K., Kraigsley, A.M., Bolikal, D., Kohn, J., and Simon, C.G. Gas-foamed scaffold gradients for combinatorial screening in 3D. J Funct Biomater **173,** 3, 2012.
6. Dalby, M.J., Gadegaard, N., Tare, R., Andar, A., Riehle, M.O., Herzyk, P., Wilkinson, C.D., and Oreffo, R.O. The control of human mesenchymal cell differentiation using nanoscale symmetry and disorder. Nat Mater **6,** 997, 2007.
7. Abbott, A. Cell culture: biology's new dimension. Nature **424,** 870, 2003.
8. Griffith, L.G., and Swartz, M.A. Capturing complex 3D tissue physiology *in vitro*. Nat Rev Mol Cell Biol **7,** 211, 2006.
9. Sachlos, E., and Czernuszka, J.T. Making tissue engineering scaffolds work. Review on the application of solid freeform fabrication technology to the production of tissue engineering scaffolds. Eur Cell Mater **5,** 29, 2003.
10. Hutmacher, D.W., Sittinger, M., and Risbud, M.V. Scaffold-based tissue engineering: rationale for computer-aided design and solid free-form fabrication systems. Trends Biotechnol **22,** 354, 2004.
11. Luo, C.J., Stoyanov, S.D., Stride, E., Pelan, E., and Edirisinghe, M. Electrospinning versus fibre production methods: from specifics to technological convergence. Chem Soc Rev **41,** 4708, 2012.
12. Hollister, S.J. Porous scaffold design for tissue engineering. Nat Mater **4,** 518, 2005.
13. Wu, C., Fan, W., Zhou, Y., Luo, Y., Gelinsky, M., Chang, J., and Xiao, Y. 3D-printing of highly uniform CaSiO3 ceramic scaffolds: preparation, characterization and *in vivo* osteogenesis. J Mater Chem **22,** 12288, 2012.
14. Kim, G.H., Ahn, S.H., Yoon, H., Kim, Y.Y., and Chun, W. A cryogenic direct-plotting system for fabrication of 3D collagen scaffolds for tissue engineering. J Mater Chem **19,** 8817, 2009.
15. Ahn, S.H., Lee, H.J., and Kim, G.H. Polycaprolactone scaffolds fabricated with an advanced electrohydrodynamic direct-printing method for bone tissue regeneration. Biomacromolecules **12,** 4256, 2011.
16. Schotel, R., Hammann, D., de Wijn, J.R., and van Blitterswijk, C.A. 3D fiber-deposited electrospun integrated scaffolds enhance cartilage tissue formation. Adv Funct Mater **18,** 53, 2008.
17. Park, S.H., Kim, T.G., Kim, H.C., Yang, D.-Y., and Park, T.G. Development of dual scale scaffolds via direct polymer melt deposition and electrospinning for applications in tissue regeneration. Acta Biomater **4,** 1198, 2008.
18. Jiankang, H., Dichen, L., Yaxiong, L., Bo, Y., Hanxiang, Z., Qin, L., Bingheng, L., and Yi, L. Preparation of chitosan–gelatin hybrid scaffolds with well-organized microstructures for hepatic tissue engineering. Acta Biomater **5,** 453, 2009.
19. Holzwarth, J.M., and Ma, P.X. Biomimetic nanofibrous scaffolds for bone tissue engineering. Biomaterials **32,** 9622, 2011.
20. Chen, G., Sato, T., Ushida, T., Ochiai, N., and Tateishi, T. Tissue engineering of cartilage using a hybrid scaffold of synthetic polymer and collagen. Tissue Eng **10,** 323, 2004.
21. Ahn, S.H., Kim, Y.B., Lee, H.J., and Kim, G.H. A new hybrid scaffold constructed of solid freeform-fabricated PCL struts and collagen struts for bone tissue regeneration: fabrication, mechanical properties, and cellular activity. J Mater Chem **22,** 15901, 2012.
22. Lee, H.J., and Kim, G.H. Cryogenically direct-plotted alginate scaffolds consisting of micro/nano-architecture for bone tissue regeneration. RSC Advances **2,** 7578, 2012.
23. Vunjak-Novakovic, G., Obradovic, B., Martin, I., Bursac, P.M., Langer, R., and Freed, L.E. Dynamic cell seeding of polymer scaffolds for cartilage tissue engineering. Biotechnol Prog **14,** 193, 1998.
24. Freed, L.E., Vunjak-Novakovic, G., and Langer, R. Cultivation of cell-polymer cartilage implants in bioreactors. J Cell Biochem **51,** 257, 1993.
25. Grayson, W.L., Marolt, D., Bhumiratana, S., Fröhlich, M., Guo, X.E., and Vunjak-Novakovic, G. Optimizing the medium perfusion rate in bone tissue engineering bioreactors. Biotechnol Bioeng **108,** 1159, 2011.
26. Sailon, A.M., Allori, A.C., Davidson, E.H., Reformat, D.D., Allen, R.J., and Warren, S.M. A novel flow-perfusion

bioreactor supports 3D dynamic cell culture. J Biomed Biotechnol **2009,** 873816, 2009.
27. Bancroft, G.N., Sikavitsas, V.I., and Mikos, A.G. Design of a flow perfusion bioreactor system for bone tissue-engineering applications. Tissue Eng **9,** 549, 2003.
28. Sikavitsas, V.I., Bancroft, G.N., and Mikos, A.G. Formation of three-dimensional cell/polymer constructs for bone tissue engineering in a spinner flask and a rotating wall vessel bioreactor. J Biomed Mater Res **62,** 136, 2002.
29. Sobral, J.M., Caridade, S.G., Sousa, R.A., Mano, J.F., and Reis, R.L. Three-dimensional plotted scaffolds with controlled pore size gradients: effect of scaffold geometry on mechanical performance and cell seeding efficiency. Acta Biomater **7,** 1009, 2011.
30. Moroni, L., Schotel, R., Hammann, D., de Wijn, J.R., and van Blitterswijk, C.A. 3D fiber deposited-electrospun integrated scaffolds enhances cartilage tissue formation. Adv Funct Mater **18,** 53, 2008.
31. Chen, Y., Bloemen, V., Impens, S., Moesen, M., Luyten, F.P., and Schrooten, J. Characterization and optimization of cell seeding in scaffolds by factorial design: quality by design approach for skeletal tissue engineering. Tissue Eng Part C **17,** 1211, 2011.
32. Yeo, M.G., Lee, H., and Kim, G.H. Three-dimensional hierarchical composite scaffolds consisting of polycaprolactone, β-tricalcium phosphate, and collagen nanofibers: fabrication, physical properties, and in vitro cell activity for bone tissue regeneration. Biomacromolecules **12,** 502, 2011.
33. Jin, G.H., and Kim, G.H., Multi-layered polycaprolactone–alginate–fucoidan biocomposites supplemented with controlled release of fucoidan for bone tissue regeneration: fabrication, physical properties, and cellular activities. Soft Matter **8,** 6264, 2012.
34. Ahn, S.H., Lee, H.J., Puetzer, J., Bonassar, L.J., and Kim, G.H. Fabrication of cell-laden three-dimensional alginate-scaffolds with an aerosol cross-linking process. J Mater Chem **22,** 18735, 2012.
35. Dai, W., Kawazoe, N., Lin, X., Dong, J., and Chen, G. The influence of structural design of PLGA/collagen hybrid scaffolds in cartilage tissue engineering. Biomaterials **31,** 2141, 2010.
36. Shor, L., Guceri, S., Chang, R., Gordon, J., Kang, Q., Hartsock, L., An, Y., and Sun, W. Precision extruding deposition (PED) fabrication of polycaprolactone (PCL) scaffolds for bone tissue engineering. Biofabrication **1,** 015003, 2009.
37. Ciardelli, G., Chiono, V., Vozzi, G., Pracella, M., Ahluwalia, A., Barbani, N., Cristallini, C., and Giusti, P. Blends of poly-(epsilon-caprolactone) and polysaccharides in tissue engineering applications. Biomacromolecules **6,** 1961, 2005.
38. Balakrishnan, B., and Jayakrishnan, A. Self-cross-linking biopolymers as injectable *in situ* forming biodegradable scaffolds. Biomaterials **26,** 3941, 2005.
39. Alsberg, E., Anderson, K.W., Albeiruti, A., Franceschi, R.T., and Mooney, D.J. Cell-interactive alginate hydrogels for bone tissue engineering. J Dent Res **80,** 2025, 2001.
40. Li, X., Liu, T., Song, K., Yao, L., Ge, D., Bao, C., Ma, X., and Cui, Z. Culture of neural stem cells in calcium alginate beads. Biotechnol Prog **22,** 1683, 2006.
41. Liu, X., and Ma, P.X. Polymeric scaffolds for bone tissue engineerin. Ann Biomed Eng **32,** 477, 2004.
42. Cyster, L., Grant, D., Howdle, S., Rose, F., Irvine, D., Freeman, D., Scotchford, C., and Shakesheff, K. The influence of dispersant concentration on the pore morphology of hydroxyapatite ceramics for bone tissue engineering. Biomaterials **26,** 697, 2005.
43. Karageorgiou, V., and Kaplan, D. Porosity of 3D biomaterial scaffolds and osteogenesis. Biomaterials **26,** 5474, 2005.
44. Discher, D.E., Janmey, P., and Wang, Y. Tissue cells feel and respond to the stiffness of their substrate. Science **310,** 1139, 2005.
45. Kim, B.S., Putnam, A.J., Kulik, T.J., and Mooney, D.J. Optimizing seeding and culture methods to engineer smooth muscle tissue on biodegradable polymer matrices. Biotechnol Bioeng **57,** 46, 1998.
46. Li, Y., Ma, T., Kniss, D.A., Lasky, L.C., and Yang, S.-T. Effects of filtration seeding on cell density, spatial distribution, and proliferation in nonwoven fibrous matrices. Biotechnol Prog **17,** 935, 2001.
47. Lutolf, M.P., and Hubbell, J.A. Synthetic biomaterials as instructive extracellular microenvironments for morphogenesis in tissue engineering. Nat Biotechnol **23,** 47, 2005.
48. Thevenot, P., Nair, A., Dey, J., Yang, J., and Tang, L. Method to analyze three-dimensional cell distribution and infiltration in degradable scaffolds. Tissue Eng Part C **14,** 319, 2008.

Address correspondence to:
GeunHyung Kim, PhD
Department of Bio-Mechatronic Engineering
College of Biotechnology and Bioengineering
Sungkyunkwan University
Suwon
South Korea

E-mail: xrdghk@gmail.com

Received: November 2, 2012
Accepted: February 8, 2013
Online Publication Date: April 10, 2013